Decoupling Optical Properties in Metallo-Supramolecular Poly(*p*-phenylene ethynylene)s

Mark Burnworth,[†] James D. Mendez,[†] Michael Schroeter,[†,§] Stuart J. Rowan,*[,†,‡] and Christoph Weder*[,†,‡]

Department of Macromolecular Science and Engineering and Department of Chemistry, Case Western Reserve University, 2100 Adelbert Road, Cleveland, Ohio 44106-7202, and Institute of Polymer Research, GKSS Research Center Geesthacht, Kantstr. 55, 14513 Teltow, Germany

Received December 6, 2007; Revised Manuscript Received January 9, 2008

ABSTRACT: The self-assembly polymerization of ditopic macromolecules through metal−ligand binding is an attractive framework for the preparation of high-molecular-weight metallo-supramolecular polymers. This approach was utilized here for the polymerization of a conjugated macromonomer (**1**) that was derived by functionalizing a low-molecular-weight poly(2,5-dialkoxy-*p*-phenylene ethynylene) (PPE) core with 2,6-bis(1′-methylbenzimidazolyl)pyridine (Mebip) ligands on the two terminal positions. To minimize electronic interactions between the PPE moieties and the metal−ligand complexes, nonconjugated hexamethylene spacers were introduced between the PPE and Mebip building blocks. The supramolecular polymerization of macromonomer **1** with equimolar amounts of Zn^{2+} or Fe^{2+} resulted in polymers, which exhibit appreciable mechanical properties (loss moduli of $[\mathbf{1}\cdot Zn(ClO_4)_2]_n$ and $[\mathbf{1}\cdot Fe(ClO_4)_2]_n$ at 25 °C are ca. 450 and 610 MPa, respectively), but on account of their dynamic, reversible nature offer the ease of processing of low-molecular-weight compounds. The optoelectronic properties of these metallopolymers are similar to those of the parent PPE and demonstrate that the functionalities of semiconducting building blocks and coordination chain extenders can be effectively decoupled by a short, nonconjugated spacer.

Introduction

There has been a lot of recent interest in the use of metal−ligand binding as the thermodynamic driving force for the self-assembly of ditopic ligands into supramolecular polymers.[1] Further to some of our preliminary work that involved the metallo-supramolecular polymerization of a small-molecule ditopic ligand,[2] we recently reported on the supramolecular polymerization of a new conjugated macromonomer that displayed appreciable mechanical properties.[3] The macromonomer was derived by functionalizing a low-molecular-weight poly(2,5-dialkoxy-*p*-phenylene ethynylene) (PPE) core as an example of conjugated polymers with well-known optoelectronic properties[4] with 2,6-bis(1′-methylbenzimidazolyl)pyridine (Mebip) ligands[5] in the two terminal positions. Polymers produced by polymerizing this macromonomer though the addition of stoichiometric amounts of Zn^{2+} or Fe^{2+} could readily be processed into films and fibers that displayed excellent mechanical properties, but the coordination to Zn^{2+} and Fe^{2+} markedly influenced the optical properties of the PPE core.[3] While the interaction with metals often provides interesting opportunities for tailoring the opto/electronic properties of ligand-containing conjugated molecules,[6,7] sometimes effects such as charge trapping or fluorescence quenching occur. For example, in the case of the aforementioned PPE-Mebip metallopolymers, the luminescence was strongly (Zn^{2+}) or even completely (Fe^{2+}) quenched.[3] With the objective to minimize electronic interactions between the PPE moieties, and noting that examples of conjugated metallopolymers in which the conjugated moieties and the organometallic motifs are electronically decoupled are limited, we here report the investigation of new supramolecular metallopolymers based on a PPE-Mebip macromonomer in which conjugated core and ligands are separated by nonconjugated hexamethylene spacers (Scheme 1).

* Corresponding authors. E-mail: stuart.rowan@case.edu, christoph.weder@case.edu.

[†] Department of Macromolecular Science and Engineering, Case Western Reserve University.

[‡] Department of Chemistry, Case Western Reserve University.

[§] GKSS Research Center Geesthacht.

Experimental Section

General Methods. All NMR spectra were recorded in $CDCl_3$ on a Varian 600 MHz NMR spectrometer; chemical shifts are expressed in ppm relative to internal TMS standard. MALDI MS spectra were recorded on a Bruker Biflex III. Dynamic mechanical thermoanalysis (DMTA) measurements were taken on a Triton Technology Tritec 2000 DMA; single frequency/strain tension (1 Hz, 0.02 mm) experiments were performed with rectangular films at a heating rate of 3 °C/min. Ultraviolet−visible (UV−vis) absorption spectra were obtained on a Perkin-Elmer Lambda 800 spectrometer. Steady-state photoluminescence (PL) spectra were acquired on a PTI C720 fluorescence spectrometer under excitation at 430 nm. The spectra were corrected for the instrument throughput and the detector response. Unless otherwise noted, solid-state absorption and PL spectra were measured on films that had been spin-coated from $CHCl_3$.

Materials. 1,4-Diethynyl-2,5-bis(octyloxy)benzene (**5**),[8] 1,4-bis-(2-ethylhexyloxy)-2,5-diiodobenzene (**6**),[8] and 2,6-bis(1′-methylbenzimidazoyl)-4-hydroxypyridine (**2**)[5a] were prepared according to literature procedures. Unless otherwise stated, all other reagents, catalysts, and solvents were purchased from Aldrich Chemical Co. or Fisher Scientific in the highest available purity and were used without further purification. Toluene was distilled from sodium under inert atmosphere, and diisopropylamine was distilled from calcium under an inert atmosphere.

2,6-Bis(1′-methylbenzimidazoyl)-4-(6-bromohexyl)pyridine (3). A suspension of freshly powdered KOH (0.37 g, 6.60 mmol) in DMSO (40 mL) was degassed by sparging with Ar for 30 min, 2,6-bis(1′-methylbenzimidazoyl)-4-hydroxypyridine (**2**) (0.938 g, 2.64 mmol) was added, and the mixture was stirred until it turned reddish. 1,6-Dibromohexane (1.42 g, 5.81 mmol) was added all at once, and the reaction mixture was stirred at 35 °C for 20 h before

10.1021/ma702712e CCC: $40.75
Published on Web 02/23/2008

Scheme 1. Synthesis and Molecular Structure of the Mebip End-Capped Macromonomer 1

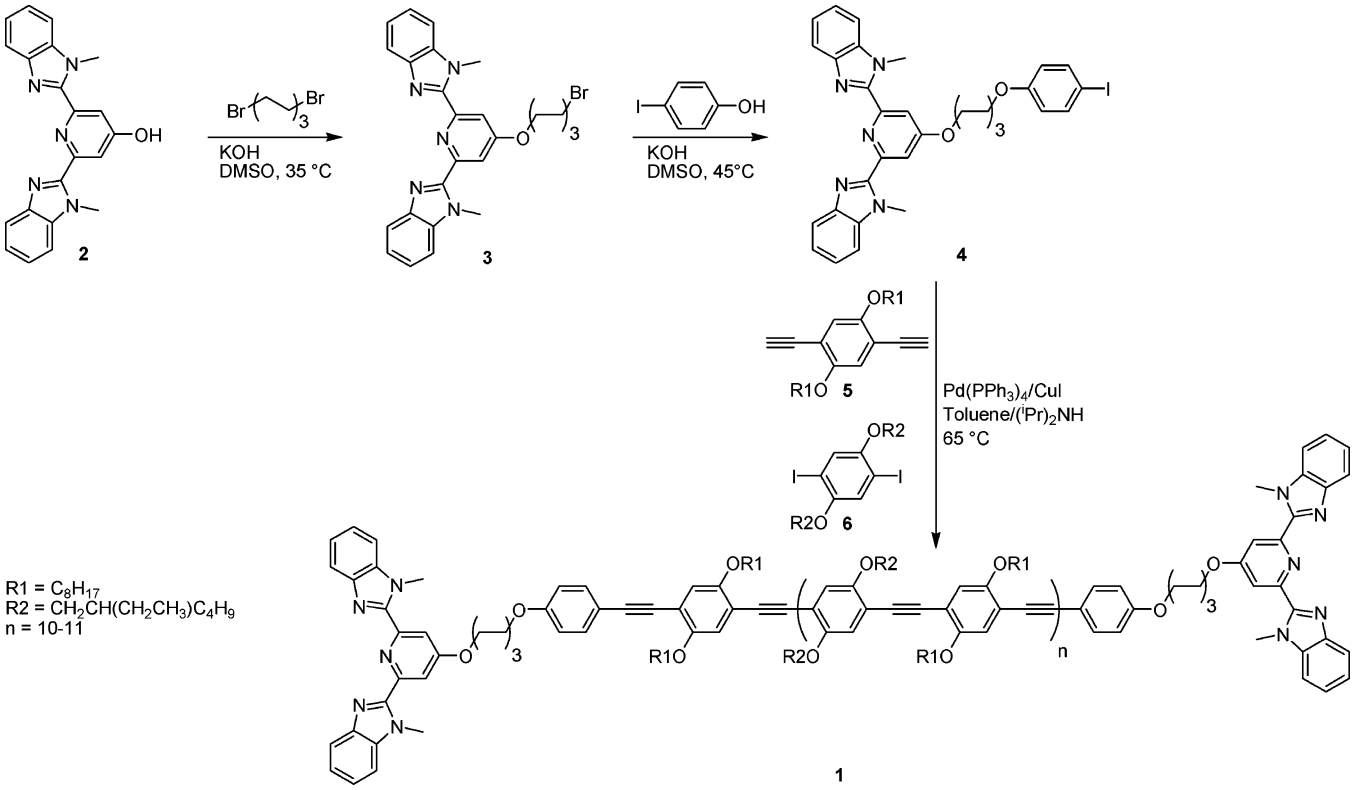

it was poured into ice water (150 mL). The resulting precipitate was collected by filtration. The crude product was purified by column chromatography (silica gel, $CHCl_3$) to yield **3** in the form of off-white needlelike crystals (0.653 g, 43%). ^{1}H NMR (600 MHz, $CDCl_3$): δ = 7.93 (s, 2H), 7.87 (d, J = 7.2 Hz, 2H), 7.46 (d, J = 7.8 Hz, 2H), 7.38 (m, 2H), 7.35 (m, 2H), 4.24 (t, J = 6.6 Hz, 2H), 4.24 (s, 6H), 3.44 (t, J = 6.6 Hz, 2H), 1.94−1.80 (m, 4H), 1.58−1.50 (m, 4H). ^{13}C NMR (100 MHz, $CDCl_3$): δ = 166.53, 165.76, 151.05, 150.38, 142.44, 137.14, 123.52, 122.79, 120.11, 111.73, 109.90, 68.36, 44.96, 33.76, 33.24, 32.52, 28.70, 28.26, 25.11. MALDI MS (matrix: HABA): m/z 518.91 [M^+], 520.91 [M^+ + 2] 1:1 intensity (required for $C_{27}H_{28}N_5OBr$ = 518.45).

2,6-Bis(1′-methylbenzimidazoyl)-4-(6-(4′-iodophenyloxy)hexyl)pyridine (4). A suspension of freshly powdered KOH (0.135 g, 2.40 mmol) in DMSO (30 mL) was degassed by sparging with Ar for 30 min, 4-iodophenol (0.424 g, 1.93 mmol) was added, and the mixture was degassed for another 5 min. **3** (0.50 g, 0.964 mmol) was added over the course of 5 min, and the mixture was stirred under Ar for 5 h at 45 °C. The reaction mixture was cooled to RT and poured into ice water (150 mL). The volume of the resulting suspension was reduced in vacuo to 1/4 of the starting volume, the white precipitate was collected by filtration, and the product was extensively washed with water and a small amount of cold DMSO. The product was dried in vacuum at RT and purified by column chromatography (silica gel, $CHCl_3$) to yield **4** as a white powder (0.391 g, 62%). ^{1}H NMR (600 MHz, $CDCl_3$): δ = 7.93 (s, 2H), 7.87 (d, J = 7.2 Hz, 2H), 7.53 (dd, J = 9 Hz, J = 2 Hz, 2H), 7.46 (d, J = 7.2 Hz, 2H), 7.38 (m, 2H), 7.35 (m, 2H), 6.68 (dd, J = 7.5 Hz, J = 2 Hz, 2H), 4.25 (t, J = 6 Hz, 2H), 4.24 (s, 6H), 3.94 (t, J = 6.6 Hz, 2H), 1.92−1.87 (m, 2H), 1.85−1.79 (m, 2H), 1.60−1.50 (m, 4H). ^{13}C NMR (100 MHz, $CDCl_3$): δ = 166.59, 151.03, 150.39, 142.42, 138.13, 137.14, 123.57, 122.85, 120.10, 118.14, 116.91, 111.80, 109.93, 82.45, 68.45, 67.86, 32.53, 29.06, 28.78, 25.69. MALDI MS: m/z 659.08 [M^+ + 2] (required for $C_{33}H_{32}N_5O_2I$ = 657.55).

Synthesis of Macromonomer 1. In a glovebox 1,4-diethynyl-2,5-bis(octyloxy)benzene (**5**) (0.200 g, 0.523 mmol), 1,4-bis(2-ethylhexyloxy)-2,5-diiodobenzene (**6**) (0.276 g, 0.471 mmol), 2,6-bis(1′-methylbenzimidazoyl)-4-(6-(4′-iodophenyloxy)hexyl)-pyridine (**4**) (0.069 g, 0.104 mmol), $Pd(PPh_3)_4$ (0.030 g, 0.026 mmol, CuI (0.005 g, 0.026 mmol), and toluene (13.5 mL) were introduced in to a reaction flask, which was subsequently equipped with a reflux condenser and connected to a Schlenk line. (iPr)$_2$NH (5.8 mL) was added, and the reaction mixture was stirred for 16 h at 65 °C. At this point an additional portion of **4** (0.034 g, 0.052 mmol) was added, and the reaction mixture was stirred at 65 °C for another 4 h. The suspension was subsequently poured hot into a saturated aqueous EDTA solution (200 mL). The flask was rinsed with $CHCl_3$, and the solution was also added to the EDTA solution, which was then stirred for 1 h. The organic layer was separated, and the aqueous layer was extracted with $CHCl_3$. The combined organic layers were washed with deionized water, and the solvent was evaporated in vacuum. The resulting solid was redissolved in $CHCl_3$, and the product was reprecipitated by adding the solution dropwise to stirred MeOH. After stirring for 1 h, the orange precipitate was filtered off and washed with boiling MeOH, EtOH, CH_3CN, cold hexanes, diethyl ether, and MeOH. The orange solid was dried overnight in vacuum at room temperature to yield macromonomer **1** (0.330 g, 78%). ^{1}H NMR (600 MHz, $CDCl_3$, 50 °C): δ = 7.96 (s, 4H, ArH end group), 7.87 (d, J = 7.2 Hz, 4H, ArH end group), 7.45 (d, J = 8.4 Hz, 8H, ArH end group), 7.38 (m, 4H, ArH end group), 7.34 (m, 4H, ArH end group), 7.01 (m, 4H, ArH), 6.88 (d, J = 8.4 Hz, 4H, ArH end group), 4.28 (t, J = 6.6 Hz, 4H, OCH_2 end group), 4.25 (s, 12H), 4.07−4.00 (m, 4H, OCH_2; 4H, OCH_2 end group), 3.98−3.90 (m, 4H, OCH_2), 1.92 (m, J = 7.2 Hz, 4H end group), 1.89−1.83 (m, 6H, CH_2, CH; 4H, CH_2 end group), 1.6−1.4 (m, 12H, CH_2; 8H, CH_2 end group), 1.4−1.2 (m, 24H, CH_2), 0.98 (t, J = 7.2 Hz, 6H), 0.89 (t, J = 7.2 Hz, 6H), 0.88 (t, J = 7.2 Hz, 6H). ^{13}C NMR (100 MHz, $CDCl_3$): δ = 165.77, 153.71, 153.42, 133.03, 123.55, 122.82, 120.15, 117.20, 116.78, 114.48, 114.38, 114.27, 111.79, 109.92, 96.33, 95.81, 94.82, 86.36, 71.88, 69.61, 39.53, 31.84, 30.59, 29.38, 29.32, 29.29, 29.11, 25.98, 23.98, 23.09, 22.66, 14.35, 11.25. X_n (determined by NMR) = 22; M_n (determined by NMR) = 8900 g/mol.

UV and PL Titrations of 1 with $Zn(ClO_4)_2$ and $Fe(ClO_4)_2$. A solution of **1** (5.0×10^{-5} M) in a mixture of $CHCl_3/CH_3CN$ (9/1 v/v) was titrated with 25 μL aliquots of either a solution of $Zn(ClO_4)_2$ (3.01×10^{-4} M) and **1** (5.0×10^{-5} M) or a solution of

Table 1. Optical Absorption and PL Emission Data of Macromonomer 1 and Supramolecular Polymers Based on Equimolar Amounts of 1 and Zn^{2+} or Fe^{2+} Ions

	solution ($CHCl_3$)		thin film	
	absorption λ_{max} (nm)	emission λ_{max}[a] (nm)	absorption λ_{max}[b] (nm)	emission λ_{max}[a,b] (nm)
1	317, 449	478, 504	320, 450, 470	492, 526, 553,[c] 580[c]
1·$Zn(ClO_4)_2$	317, 356, 449	478, 504	320, 358, 450, 467	488, 523, 560[c]
1·$Fe(ClO_4)_2$	317, 356, 449, 573	478, 504	320, 358, 450, 467, 573	488, 520

[a] Excitation at 430 nm. [b] Spin-coated from $CHCl_3$ solution. [c] Dependent on sample thickness and thermal history.

$Fe(ClO_4)_2$ (3.16×10^{-4} M) and **1** (5.0×10^{-5} M) in the same solvent mixture. The addition was done incrementally; after each addition of an aliquot of the metal solution the samples were characterized by UV and PL spectroscopy. The M_n of **1** was calculated from the metal ion titration experiments (cf. Figures 2 and 3), assuming fully end-capped macromonomer; $M_n \approx 8000$ g/mol for both $Zn(ClO_4)_2$ and $Fe(ClO_4)_2$, which corresponded to a $X_n \approx 19.5$.

Typical Sample Preparation of Metallo-Supramolecular Polymers [1·MX_2]$_n$. A solution of $Zn(ClO_4)_2$ in CH_3CN (223 μL of a 0.0343 M solution, 7.67 μmol) was added to a stirred solution of **1** (61.38 mg, 7.67 μmol) in $CHCl_3$ (2 mL), to produce a solution with a 1:1 Zn^{2+}:**1** molar ratio. For this experiment, the M_n determined by UV titration with $Zn(ClO_4)_2$ was employed (M_n = 8000 g/mol). Immediately upon addition, the mixture became highly viscous. A portion of the solution was transferred to a cylindrical aluminum film caster (diameter 5.4 cm) with Teflon base. The solvent was slowly evaporated at RT over the course of 24 h, and the resulting film was subsequently dried in vacuum at RT for an additional 24 h. The resulting orange film (diameter: 5.2 cm; thickness: ca. 40 μm) was cut into smaller pieces for analysis by DMTA and PL spectroscopy. Films of a thickness of less than 2.0 μm were prepared by spin-coating $CHCl_3$ solutions of the polymer prepared as described above (concentration ca. 7 mg/mL) onto glass slides.

LED Fabrication and Testing. Single-layer LEDs were manufactured under ambient conditions by spin-coating $CHCl_3$ solutions (ca. 7 mg/mL) of the metallo-supramolecular polymer [**1**·$Zn(ClO_4)_2$]$_n$ or [**1**·$Fe(ClO_4)_2$]$_n$ onto indium−tin oxide-coated glass slides. The films were not further dried and had a thickness of between 0.5 and 1.5 μm. Aluminum was deposited as the cathode with a Denton Vacuum Bench Top Tubo III metal evaporator. The current−voltage characteristics were measured with a Keithley 2410 1100 V source meter. Electroluminescence spectra were measured at the peak output (20−30 V) of the LED with an Ocean Optics ACD1000-USB spectrometer and are not corrected. Brightness was measured with a Minolta LS-100 luminance meter.

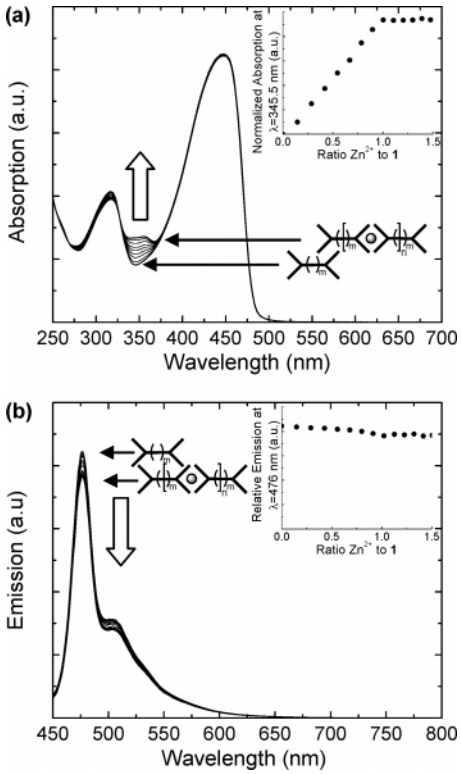

Figure 1. (a) UV−vis absorption spectra acquired upon titration of **1** (50 μM) in $CH_3CN/CHCl_3$ (1/9 v/v) with $Zn(ClO_4)_2$. The inset shows the absorption at 345.5 nm as a function of Zn^{2+}:**1** ratio. (b) PL emission spectra acquired under excitation at 430 nm upon titration of **1** (50 μM) in $CH_3CN/CHCl_3$ (1/9 v/v) with $Zn(ClO_4)_2$. The inset shows the emission at 476 nm as a function of Zn^{2+}:**1** ratio.

Results and Discussion

Synthesis of Macromonomer 1. The 2,6-bis(1′-methylbenzimidazoyl)pyridine (Mebip) end-capped PPE macromonomer **1** was prepared according to standard protocols[3,8] via the Sonogashira cross-coupling reaction of aryl acetylene **5** and aryl iodide **6**, using the Mebip derivative 2,6-bis(1′-methylbenzimidazolyl)-4-ethynylpyridine (**4**) as an end-capper (Scheme 1). The end-capper was synthesized by reacting the hydroxy group of 2,6-bis(1′-methylbenzimidazoyl)-4-hydroxypyridine[5a] (**2**) with an excess of 1,6-dibromohexane in the presence of potassium hydroxide to yield 2,6-bis(1′-methylbenzimidazoyl)-4-(6-bromohexyl)pyridine (**3**). Further reaction of the remaining bromomethyl group in **3** with 4-iodophenol afforded **4** in good yield. In order to ensure good solubility of the targeted PPE, monomers featuring octyloxy (**5**) and 2-ethylhexyloxy side chains (**6**)[8] were employed. The number-average degree of polymerization, X_n, was limited to a target value of 20 by slightly offsetting the molar ratio of the two bifunctional monomers **5** and **6**. According to standard procedure,[4,8] the polycondensation reaction was performed using $Pd(PPh_3)_4$/CuI as the catalyst system in a mixture of toluene and diisopropylamine. A small excess of the Mebip-end-capper **4** was added toward the end of the reaction, with the objective to completely end-cap macromonomer **1** with Mebip ligands. To ensure removal of any Mebip-binding residues of the Pd and Cu catalysts, the workup of **1** involved rigorous extraction with aqueous EDTA and several organic solvents (see Experimental Section for details). Macromonomer **1**, which was completely soluble at concentrations of at least ≈30 mg/mL in solvents such as $CHCl_3$, toluene, and THF, was characterized to satisfaction by ^1H and ^{13}C NMR spectroscopy. The number-average degree of polymerization, X_n, of ≈22 (number-average molecular weight, M_n, ≈8900 g/mol), determined by ^1H NMR end-group analysis, was in good agreement with a value of $X_n \approx 19.5$ ($M_n \approx 8000$ g/mol) determined by the UV titration of **1** with Zn^{2+} or Fe^{2+} (vide infra). The latter value was used for the stoichiometric calculations when preparing metallo-supramolecular materials.

Optical Properties of Macromonomer 1. The optical properties of macromonomer **1** were investigated in both solution and solid state; all spectroscopic data are summarized in Table 1, and solution spectra are shown in Figure 1. The solution absorption spectrum reveals two main bands associated with the conjugated polymer backbone; the stronger absorption band centered at 449 nm is related to the $\pi-\pi^*$ transition, while

the weaker band centered at 317 nm is due to the n−π* transition. Macromonomer **1** is highly fluorescent. The emission spectrum exhibits two bands around 478 and 504 nm that are consistent with $\pi-\pi$* fluorescence. The Mebip end groups do not appear to significantly alter the electronic properties, as a comparison between the optical data of **1** and poly(2,5-dioctyloxy-*p*-phenylene ethynylene) without the Mebip end groups[8] reveals. Spin-coating macromonomer **1** from $CHCl_3$ solution produced homogeneous films of good optical quality. Compared to solution, the absorption spectrum of a film of macromonomer **1** displays a new sharp feature at 470 nm, along with a small red shift; the $\pi-\pi$* and n−π* transitions now appear around 455 and 320 nm. The thin-film emission spectrum is also red-shifted and significantly broadened (Table 1); with increasing sample thickness and/or upon annealing above the glass transition temperature an additional peak at ca. 580 nm can be observed (Supporting Information). These features are characteristic of intermolecular interactions among the PPE molecules and depend on the degree of order, which is influenced by the processing conditions and/or thermal history of the sample.[8−10]

Supramolecular Polymerization of Macromonomer 1 with Zn^{2+} and Fe^{2+}. The formation of metallo-supramolecular polymers $[\mathbf{1}\cdot MX_2]_n$ was achieved by the addition of metal salts dissolved in CH_3CN to a $CHCl_3$ solution of macromonomer **1**. A variety of metal ions display appropriate interactions (i.e., large equilibrium constant and rapid complexation kinetics) that allow for supramolecular polymerization utilizing the Mebip ligand. We employed Zn^{2+} and Fe^{2+} in this study to explore the influence of these metals on the resulting metallopolymers and to compare them with previously investigated materials.[2,3,6d] Zn^{2+} features a fully occupied d-orbital ($3d^{10}$) and is a prototype for metals that show hardly any tendency for metal-to-ligand charge transfer (MLCT) with imine-type ligands.[11] We previously observed in several material systems that the optical properties of phenylene ethynylene chromophores with imine ligands display significant changes upon complexation to Zn^{2+}, usually a significant reduction of the PL intensity and the development of orange luminescence.[2,3,6d] We speculated that these changes might be suppressed by the introduction of a spacer between the chromophore and the ligand. By contrast, Fe^{2+} is well-known to form pronounced MLCT complexes and to act as a strong fluorescence quencher.[12] We assumed that electronic interactions with the PPE backbone could be substantially reduced through the spacer but anticipated PL quenching through Förster-type energy transfer between the PPE and the MLCT complex (vide infra).

The metallopolymerization of macromonomer **1** with either of these metals in a 1:1 molar ratio caused the expected visual changes. The addition of a CH_3CN solution of $Zn(ClO_4)_2$to a $CHCl_3$ solution of **1** (ca. 30 mg/mL) resulted in an instantaneous and significant viscosity increase, while the color of the solution remained virtually unchanged. The addition of a CH_3CN solution of $Fe(ClO_4)_2$, dissolved into a $CHCl_3$ solution of **1** (ca. 30 mg/mL), led to the rapid formation of a gel, which could be converted into a viscous purple solution upon addition of more $CHCl_3$ to dilute the concentration of the solution to ca. 20 mg/mL. A portion of these solutions were used for solution-casting to produce orange (Zn^{2+}) or purple (Fe^{2+}) films. Even at a thickness of only ca. 40 μm these films displayed appreciable mechanical properties (vide infra), demonstrating unequivocally that the resulting metallopolymers—very much in contrast to the neat macromonomer **1** and a poly(2,5-dioctyloxy-*p*-phenylene ethynylene) of similar X_n but without the Mebip end groups—offer considerable mechanical strength and flexibility. The remainder of the solutions was reduced in vacuum and could be redissolved in $CHCl_3$,[13] and the resulting solutions were employed to produce thin films for optical experiments by spin-coating (thickness ca. 1 μm).

Optical Properties of $[\mathbf{1}\cdot Zn(ClO_4)_2]_n$ and $[\mathbf{1}\cdot Fe(ClO_4)_2]_n$. To monitor the metal-mediated self-assembly processes of **1** and to elucidate the effect of the spacer between Mebip ligand and PPE chromophore, $Zn(ClO_4)_2$ (Figure 1) and $Fe(ClO_4)_2$ (Figure 2) were titrated into solutions of **1**, and the resulting products were analyzed by means of UV−vis absorption and PL spectroscopy. The precipitation of high-molecular-weight macromolecules at higher concentrations dictated that the titration experiments were performed at rather low concentrations (50 μM); these conditions favor the formation of oligiomeric species as opposed to high-molecular-weight aggregates. Figure 1a reveals that the absorption arising from the PPE backbone is hardly changed upon addition of Zn^{2+}. However, a small increase of the absorption in the regime of 330−375 nm, and a slight decrease of the absorption in the regime of 270−325 nm, can be observed, which is interpreted with the formation of Zn−Mebip complexes.[2a] The inset of Figure 1a, which displays the absorption at 345.5 nm as a function of $[Zn^{2+}]$, shows that this transition intensifies linearly with the Zn^{2+} concentration. The molecular weight of the sample, calculated by correlating the point where the absorption at 345.5 nm levels off to a Zn^{2+}:**1** ratio of 1:1, was determined to be ca. 8000 g/mol, which is in good agreement with the ^1H NMR end-group analysis. This behavior is evidence for the formation of a metallo-supramolecular complex of the form $[\mathbf{1}\cdot Zn(ClO_4)_2]_n$, as is required for the formation of the supramolecular polymer. Figure 1b demonstrates that, as intended, the PL emission characteristics of **1** remain virtually unchanged upon addition of Zn^{2+}; the spectral features remain identical while the emission intensity experiences only a minor reduction (ca. 90% of the original value). This behavior is in marked contrast to that of a previously investigated metallopolymer of an otherwise identical structure, but without the hexamethylene spacers between the PPE core and the Mebip ligands.[3] In that case the photoluminescence was almost completely quenched and exhibited a significant bathochromic shift, as a result of strong electronic coupling between the PPE-based core and the Mebip−Zn^{2+} termini and efficient energy migration to the latter sites.[14] Thus, the hexamethylene spacers between the conjugated backbone and the Mebip groups indeed provide efficient "optical insulation" and decouple the optical properties of the PPE backbone from the Mebip−Zn^{2+} complexes, which now merely function as "chain extenders".

The addition of Fe^{2+} to macromonomer **1** causes, at first glance, similar optical changes as observed for the addition of Zn^{2+}. As in the case of Zn^{2+}, the absorption slightly increases in the range between 330 and 375 nm and decrease in the range between 270 and 325 nm (Figure 2a). The changes scale linearly with the Fe^{2+} concentration and level off at a Fe^{2+}:**1** ratio of about 1:1. At the same time, a weak but characteristic metal-to-ligand charge-transfer (MLCT) absorption band centered at ca. 575 nm can be observed, which is concomitant with the formation of a 2:1 Mebip−Fe^{2+} complex[15,16] and indicative of a supramolecular polymer of the structure $[\mathbf{1}\cdot Fe(ClO_4)_2]_n$. Also in this case the features of the PL spectrum (Figure 2b) remain completely unchanged, and the polymer remains highly luminescent upon introduction of Fe^{2+}—unlike virtually all other previously investigated supramolecular materials comprising Fe^{2+}. However, the emission intensity does decrease linearly with increasing Fe^{2+} concentration to level off at ca. 40% of

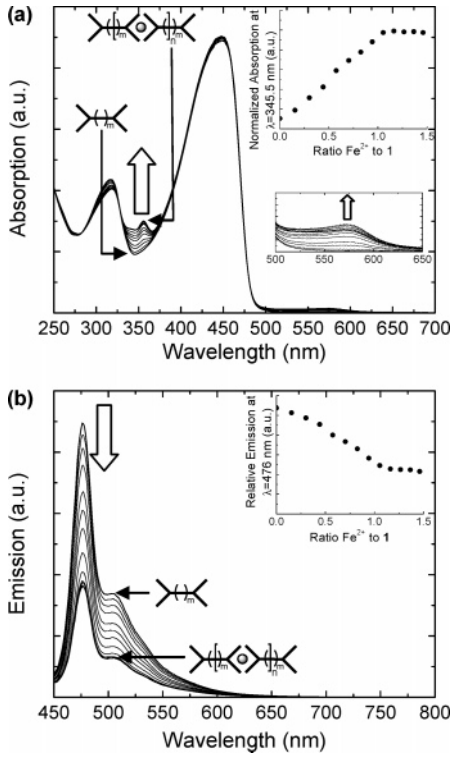

Figure 2. (a) UV−vis absorption spectra acquired upon titration of **1** (50 μM) in $CH_3CN/CHCl_3$ (1/9 v/v) with $Fe(ClO_4)_2$. The top inset shows the absorption at 345.5 nm as a function of Fe^{2+}:**1** ratio; the bottom inset is a 30× magnification showing the MLCT band. (b) PL emision spectra acquired under excitation at 430 nm upon titration of **1** (50 μM) in $CH_3CN/CHCl_3$ (1/9 v/v) with $Fe(ClO_4)_2$. The inset shows the emission at 476 nm as a function of Fe^{2+}:**1** ratio.

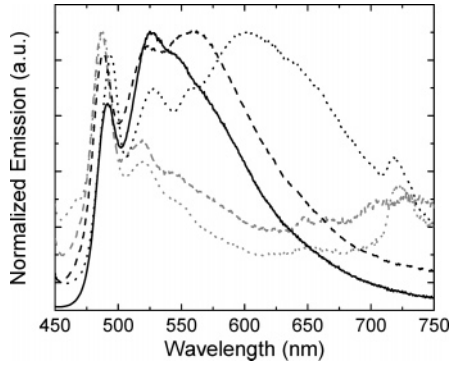

Figure 3. Normalized PL emission spectra of thin solid films: spin-coated neat macromonomer **1** (black solid line), spin-coated [**1**·$Zn(ClO_4)_2]_n$ (black dashed line), solution-cast [**1**·$Zn(ClO_4)_2]_n$ (black dotted line), solution-cast [**1**·$Zn(ClO_4)_2]_n$ (gray dashed line), and solution-cast [**1**·$Fe(ClO_4)_2]_n$ (gray dotted line).

its original value at a ligand:metal ratio of ca. 2:1. This behavior suggests weak Förster-type energy transfer between the PPE core and the Mebip−Fe^{2+} end groups, which is enabled by the overlap of the emission of the PPE core with the absorption of the Mebip−Fe^{2+} MLCT band and provides pathways for nonradiative exciton decay. It appears possible to further minimize the effect by extending the spacer length and minimizing the overlap integral by appropriate molecular engineering.

The optical properties of spin-coated thin films of **1** and [**1**·$Zn(ClO_4)_2]_n$ are very similar (Figure 3), indicating that also in the solid state the optical insulation between the PPE backbone and the Mebip−Zn^{2+} complexes is maintained. The spectra show rather narrow, well-resolved emission bands that are characteristic for disordered samples which lack significant long-range order and specific intermolecular interactions.[8] The aggregation band of [**1**·$Zn(ClO_4)_2]_n$ at ca. 580 nm is more pronounced than in the case of **1**. The relative magnitude of this band increases with sample thickness (Supporting Information), as is evident from the comparison of a spin-coated thin and solution-cast thick film (Figure 3). The PL spectrum of solution-cast samples is overwhelmed by the appearance of this new band, which produces a significant red shift (Figure 3). This very significant influence of the processing condition is consistent with an increased degree of long-range order[17] that is facilitated by slower solvent evaporation and mirrors the findings of studies in which samples of neat PPE (without Mebip) were either processed under slow solvent evaporation or annealed.[8−10]

Also, the optical properties of spin-coated films of [**1**·$Fe(ClO_4)_2]_n$ correlate nicely with those of the parent PPE **1**. The absorption spectrum additionally shows the MLCT band at 575 nm (Supporting Information). The PL spectrum resembles that of **1** even more closely than that of [**1**·$Zn(ClO_4)_2]_n$. Even for thicker films no pronounced low-energy band emerges, which can be attributed to the absorption of the MLCT which occurs at the same wavelength. Inspection of films of similar thickness under 365 nm UV light as well as PL emission spectra show qualitatively that the photoluminescence quantum efficiency of [**1**·$Fe(ClO_4)_2]_n$ films is lower than those of the neat macromonomer and [**1**·$Zn(ClO_4)_2]_n$. This is consistent with the solution study (vide supra) and explained with energy transfer to the MLCT sites where nonradiative energy dissipation occurs.

In order to explore how the presence of the Mebip−Zn^{2+} or Mebip−Fe^{2+} complexes influences the performance of the metallopolymers vis-à-vis the parent PPE, we prepared single-layer light-emitting diodes (LEDs) based on [**1**·$Zn(ClO_4)_2]_n$ or [**1**·$Fe(ClO_4)_2]_n$, ITO, and Al. The response of these most simple, by no means optimized, devices was compared with that of a single-layer device based on a polymer corresponding to the core employed here, i.e., a PPE featuring *n*-octyloxy and 2-ethylhexyloxy side chains in an alternating pattern (EHO−OPPE).[18] The *I*−*V* curves of LEDs based on [**1**·$Zn(ClO_4)_2]_n$ show typical rectifying behavior (Figure 4b) with an onset voltage of ca. 1.25 MV/cm and a maximum brightness of ca. 29 cd/m^2. These data are indeed very similar to those of a comparable EHO−OPPE device (onset voltage of ca. 1.10 MV/cm and maximum brightness of ca. 22 cd/m^2). The LEDs based on [**1**·$Fe(ClO_4)_2]_n$ show a slightly higher onset voltage (ca. 1.40 MV/cm) and a significantly lower maximum brightness of ca. 10 cd/m^2, consistent with the observed energy transfer to the Fe−Mebip complexes and nonradiative energy dissipation. The devices were found to emit green-yellow to yellow-orange light (Figure 4a) with an emission maximum at 570 nm for the [**1**·$Zn(ClO_4)_2]_n$ and 495 nm for the [**1**·$Fe(ClO_4)_2]_n$. The emission spectra that nicely match the PL spectra, indicating that indeed the same excited states are responsible for the respective emission processes. These devices are, of course, by no means optimized, but the comparative preliminary experiment suggests that the Mebip−Zn^{2+} and Mebip−Fe^{2+} complexes do not negatively impact the materials performance in these LEDs compared to the parent, metal-free PPE.

Mechanical Properties of [1·Zn(ClO$_4$)$_2$] and [1·Fe(ClO$_4$)$_2$]$_n$. [**1**·$Zn(ClO_4)_2]_n$ and [**1**·$Fe(ClO_4)_2]_n$ displayed very good film-forming characteristics, and objects produced from these polymers displayed appreciable mechanical properties (Figure 5, Supporting Information)—quite in contrast to the parent macromonomer, which is rather brittle and does not have

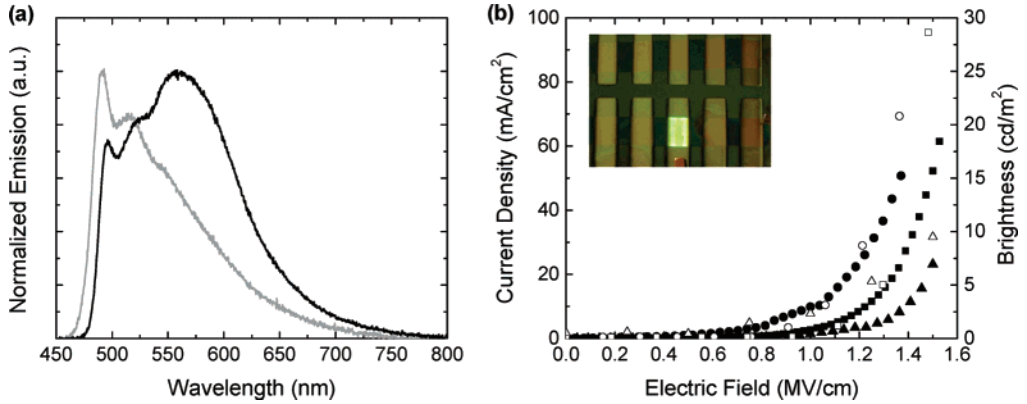

Figure 4. (a) Electroluminescence spectra of [**1**·Zn(ClO$_4$)$_2$]$_n$ (black line) and [**1**·Fe(ClO$_4$)$_2$]$_n$ (gray line). (b) Typical $I-V$ curve and brightness for a linear PPE (solid circles, hallow circles), a [**1**·Zn(ClO$_4$)$_2$]$_n$ (solid squares, hollow squares), and [**1**·Fe(ClO$_4$)$_2$]$_n$ (solid triangles, hollow triangles). The inset shows a picture of a typical [**1**·Zn(ClO$_4$)$_2$]$_n$ device under ambient illumination.

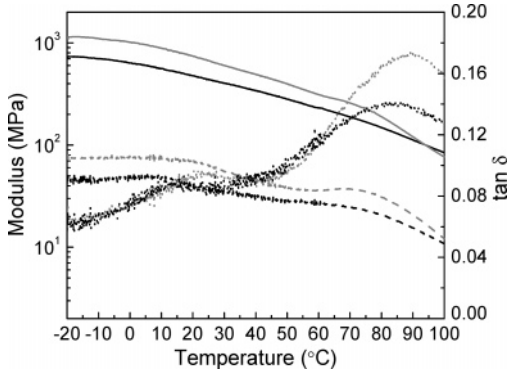

Figure 5. Dynamic mechanical thermoanalysis (DMTA) traces of [**1**·Zn(ClO$_4$)$_2$]$_n$ (black) and [**1**·Fe(ClO$_4$)$_2$]$_n$ (solid): storage modulus (solid line), loss modulus (dashed line), and tan δ (dotted line). Experiments were conducted under N_2 at a heating rate of 3 °C/min and a frequency of 1 Hz.

the ability to form self-supporting films. The mechanical properties of [**1**·Zn(ClO$_4$)$_2$]$_n$ and [**1**·Fe(ClO$_4$)$_2$]$_n$ were investigated in detail by means of dynamic mechanical thermoanalysis (DMTA, Figure 5). Experiments were conducted in a temperature range of −20 to 100 °C, i.e., in a regime in which both the PPE core[19] and the Mebip−Zn^{2+} complexes[3] are thermally stable. Data reported represent averages of three samples for each metallopolymer. The loss and storage moduli of [**1**·Zn(ClO$_4$)$_2$]$_n$ were determined to be ca. 770 and ca. 48 MPa at −20 °C and ca. 450 and ca. 40 MPa at 25 °C, respectively. The loss and storage moduli of [**1**·Fe(ClO$_4$)$_2$]$_n$ were slightly higher: ca. 1090 and ca. 66 MPa at −20 °C and ca. 610 and ca. 56 MPa at 25 °C, respectively. This difference is consistent with the higher binding constant of Fe^{2+}, which results in a higher molecular weight of [**1**·Fe(ClO$_4$)$_2$]$_n$. The effect may also reflect a slightly higher long-range order of the iron-based metallopolymer, although this aspect was not investigated. Interestingly, the room temperature moduli are significantly higher than those of the previously investigated metallopolymers of otherwise identical structure, but without the hexamethylene spacers between the PPE core and the Mebip ligands.[3,20] It appears that the higher modulus of the present materials is either related to the "flexible" coupling of the rigid PPE segments with the metallo-supramolecular motifs, which may mediate the polydisperse nature of the rigid segment in allowing for a better phase separation of PPE and metal−ligand segments, and/or that the different substitution of the Mebip ligand (alkyloxy vs ethynyl-PPE) leads to different binding strengths and/or kinetics. While further investigation of this observation is outside the scope of this paper, we note that detailed studies probing this phenomenon would be important to the development of metallo-supramolecular materials. The DMTA traces show a significant decrease of the moduli with increasing temperature. The tan δ curve suggest a thermal transition around ca. 85 °C, which in view of the striking similarity to the traces of a high-molecular-weight poly(*p*-2,5-dialkoxyphenylene ethynylene) ($M_n \sim 83\,000$ g mol^{-1})[19] and the previously reported PPE metallopolymers,[3] we assign to a glass transition.

Conclusions

In summary, we have shown that flexible, mechanically stable films that show photo- and electroluminescent properties can be easily access by using metallo-supramolecular polymers. In this system the ligand (Mebip) end groups are electronically decoupled from the conjugated poly(*p*-phenylene ethynylene) core through the use of a hexamethylene alkyl spacer. Thus, addition of either Zn^{2+} or Fe^{2+} salts to the macromonomer results in a self-assembled polymer in which the metal ligand complexes are not directly coupled to the light-emitting core, dramatically reducing its ability to quench the cores fluorescence, as is seen in related systems in which the ligands are in conjugation with the polymer backbone.[3] Thus, it appears that the use of such supramolecular polymerizations offers a broadly useful means to attain mechanically robust inorganic/organic hybrid materials without significantly altering the optoelectronic properties associated with the macromolecular core.

Acknowledgment. This material is based upon work supported by the U.S. Army Research Office (DAAD19-03-1-0208 and W911NF-06-1-0414) and the National Science Foundation under Grants CAREER-CHE-0133164, CHE-0704026, and DMR-0215342. We are also grateful for financial support through a European Union Marie Curie Outgoing Fellowship for M.S. (Project CONDPOLS-2, Contract No. 8715). We acknowledge fruitful discussions with Dr. Daniel Knapton.

Supporting Information Available: ^{1}H NMR spectrum of **1**, UV−vis spectrum of spin-coated films of the neat macromonomer **1**, Zn^{2+}:**1**, and Fe^{2+}:**1**, thickness dependence of PL emission spectra of **1** and Zn^{2+}:**1**, thermal and processing dependence on PL emission spectra of **1**, and pictures of Zn^{2+}:**1** under ambient illumination and under UV light. This material is available free of charge via the Internet at http://pubs.acs.org.

References and Notes

(1) For recent reviews see: (a) Lohmeijer, B. G. G.; Schubert, U. S. *J. Polym. Sci., Part A: Polym. Chem.* **2003**, *41*, 1413. (b) Dobrawa, R.; Würthner, F. *J. Polym. Sci., Part A: Polym. Chem.* **2005**, *43*, 4981−

4995. (c) Holliday, B. J.; Swager, T. M. *Chem. Commun.* **2005**, 23. (d) Friese, V. A.; Kurth, D. G. *Coord. Chem. Rev.* **2008**, *252*, 199.
(2) (a) Iyer, P. K.; Beck, J. B.; Weder, C.; Rowan, S. J. *Chem. Commun.* **2005**, 319. (b) Knapton, D.; Burnworth, M.; Rowan, S. J.; Weder, C. *Angew. Chem., Int. Ed.* **2006**, *45*, 5825. (c) Burnworth, M.; Rowan, S. J.; Weder, C. *Chem.—Eur. J.* **2007**, *13*, 7828.
(3) (a) Knapton, D.; Rowan, S. J.; Weder, C. *Macromolecules* **2006**, *39*, 651. (b) Burnworth, M.; Knapton, D.; Rowan, S. J.; Weder, C. *J. Inorg. Organomet. Polym. Mater.* **2007**, *17*, 40, 91.
(4) Voskerician, G.; Weder, C. *Adv. Polym. Sci.* **2005**, *177*, 209.
(5) (a) Beck, J. B.; Rowan, S. J. *J. Am. Chem. Soc.* **2003**, *125*, 13922. (b) Zhao, Y.; Beck, J. B.; Rowan, S. J.; Jamieson, A. M. *Macromolecules* **2004**, *37*, 3529. (c) Rowan, S. J.; Beck, J. B. *Faraday Discuss.* **2005**, *128*, 43. (d) Beck, J. B.; Ineman, J. M.; Rowan, S. J. *Macromolecules* **2005**, *38*, 5060. (e) Knapton, D.; Rowan, S. J.; Weder, C. *Macromolecules* **2006**, *39*, 4069. (f) Weng, W.; Beck, J. B.; Jamieson, A. M.; Rowan, S. J. *J. Am. Chem. Soc.* **2006**, *128*, 11663. (g) Weng, W.; Jamieson, A. M.; Rowan, S. J. *Tetrahedron* **2007**, *63*, 7419.
(6) (a) Huber, C.; Bangerter, F.; Caseri, W.; Weder, C. *J. Am. Chem. Soc.* **2001**, *123*, 3857. (b) Kokil, A.; Shiyanovskaya, I.; Singer, K. D.; Weder, C. *J. Am. Chem. Soc.* **2002**, *124*, 9978. (c) Kokil, A.; Huber, C.; Caseri, W.; Weder, C. *Macromol. Chem. Phys.* **2003**, *204*, 40. (d) Kokil, A.; Yao, P.; Weder, C. *Macromolecules* **2005**, *38*, 3800. (e) Weder, C. *Chem. Commun.* **2005**, 5378. (f) Weder, C. *J. Inorg. Organomet. Polym. Mater.* **2006**, *16*, 1.
(7) See for example: (a) Encinas, S.; Flamigni, L.; Barigelletti, F.; Constable, E. C.; Housecroft, C. E.; Schofield, E.; Figgemeier, E.; Fenske, D.; Neuburger, M.; Vos, J. G.; Zehnder, M. *Chem.—Eur. J.* **2002**, *8*, 137. (b) Dobrawa, R.; Lysetska, M.; Ballester, P.; Grüne, M.; Würthner, F. *Macromolecules* **2005**, *38*, 1315. (c) Chen, Y.-Y.; Tao, Y.-T.; Lin, H.-C. *Macromolecules* **2006**, *39*, 8559. (d) Gerhardt, W. W.; Zucchero, A. J.; South, C. R.; Bunz, U. H. F.; Weck, M. *Chem.—Eur. J.* **2007**, *13*, 4467. (e) Han, F. S.; Higuchi, M.; Kurth, D. G. *Adv. Mater.* **2007**, *19*, 3928.
(8) (a) Weder, C.; Wrighton, M. S. *Macromolecules* **1996**, *29*, 5157. (b) Dellsperger, S.; Dötz, F.; Smith, P.; Weder, C. *Macromol. Chem. Phys.* **2000**, *201*, 192.
(9) (a) Halkyard, C. E.; Rampey, M. E.; Kloppenburg, L.; Studer-Martinez, S. L.; Bunz, U. H. F. *Macromolecules* **1998**, *31*, 8655. (b) Levitus, M.; Schmieder, K.; Ricks, H.; Shimizu, K. D.; Bunz, U. H. F.; Garcia-Garibay, M. A. *J. Am. Chem. Soc.* **2001**, *123*, 4259.
(10) Li, H.; Powell, D. R.; Hayashi, R. K.; West, R. *Macromolecules* **1998**, *31*, 52.
(11) Jaeger, F. M.; van Dijk, J. A. *Z. Anorg. Chem.* **1938**, *227*, 273.
(12) Dobrawa, R.; Wuerthner, F. *Chem. Commun.* **2002**, 1878.
(13) Note that redissolution of the dried metallopolymer, especially the [**1**·$Fe(ClO_4)_2$]$_n$, was a time-consuming process, and direct processing of the original metallopolymer solution is clearly a sensible alternative. However, we found it convenient to first prepare and store this metallopolymer in a solid form, of which portions could be employed for the various processing experiments described.
(14) (a) Zhou, Q.; Swager, T. M. *J. Am. Chem. Soc.* **1995**, *117*, 12593. (b) Swager, T. M. *Acc. Chem. Res.* **1998**, *31*, 201.
(15) Krumholz, P. *Inorg. Chem.* **1965**, *4*, 612.
(16) El-ghayoury, A.; Schenning, A. P. H. J.; Meijer, E. W. *J. Polym. Sci., Part A: Polym. Chem.* **2002**, *40*, 4020.
(17) Note that the changes on the high-energy end of the spectrum also reflect increasing internal absorption for thicker samples.
(18) (a) Montali, A.; Smith, P.; Weder, C. *Synth. Met.* **1998**, *97*, 123. (b) Schmitz, C.; Pösch, P.; Thelakkat, M.; Schmidt, H.-W.; Montali, A.; Feldman, K.; Smith, P.; Weder, C. *Adv. Funct. Mater.* **2001**, *11*, 41.
(19) Steiger, D.; Smith, P.; Weder, C. *Macromol. Rapid Commun.* **1997**, *18*, 643.
(20) To unequivocally exclude experimental errors, the previously reported materials were resynthesized and remeasured and the mechanical data reported in ref 2 were confirmed.

MA702712E